Pulse shaping and processing by cascaded third-harmonic generation in quasiperiodic optical superlattices

Yi-qiang Qin, Sing-hai Tang, Hong Su, and Hong-chen Guo
Department of Physics, National University of Singapore, 117542, Singapore
(Received 20 October 2003; revised manuscript received 20 May 2004; published 18 October 2004)

Theoretical investigation on the temporal and spectral distributions of cascade third harmonic generation in a quasiperiodically optical superlattice is presented. Pulse shaping and integrated energy conversion are studied, for both input transform-limited and chirped pulses, as well as for both phase matched and phase mismatched configurations. Not only the phase mismatch between the center frequencies of the fundamental and harmonic pulses but also the group velocity mismatches (GVM) among the interacting pulses are considered. The pulse shaping features consisting of a multiplicity in phase and amplitude are observed. Additionally, there are some interesting phenomena in harmonic energy conversion, which provide more flexibility for harmonic generations in the ultrashort pulse range.

DOI: 10.1103/PhysRevA.70.045803 PACS number(s): 42.65.Ky, 42.65.Re, 42.70.Mp, 77.84.Dy

Optical phenomena induced by second order nonlinearity have been investigated intensively due to their potential revolutions for laser frequency conversions. Much research has been conducted on subjects such as second harmonic generation (SHG), optical parametric amplification and oscillation, wavelength division multiplexing and cascaded optical nonlinearity. Recently considerable interest has been focused on high harmonic generation which has been widely used to extend the laser wavelength to the ultraviolet (UV) and extreme UV range. Quasi-phase-matched (QPM) third harmonic generation (THG) has been demonstrated through $\chi^{(3)}$ in a simple silica structure [1]. Continuous wave (cw) frequency tripling by simultaneous three-wave mixing has been realized in a periodically poled $LiNbO_3$ (LN) crystal [2] and UV 355 nm THG has been observed in a LN waveguide [3]. In particular, QPM THG induced by cascaded SHG and sum frequency generation (SFG) in a quasiperiodic structure has been realized with high conversion efficiency [4].

Although most treatments to date have considered the case of tunable cw harmonic generation, the interests in using ultrashort pulse lasers to generate equally short pulses have strongly increased in recent years. It is envisaged that the large output power of high harmonic generation can be achieved more readily with the use of high peak pump power densities from the pulsed lasers. Furthermore, it has been widely reported that ultrafast pulse shaping was applied to many fields such as ultrafast nonlinear fiber optics [5], optical communication networks [6], chirped pulse amplification [7], the coherent control of atomic and molecular processes [8], as well as coherent control in a chemical reaction [9].

For ultrafast pulse shaping, the most extensive method carried out is by means of Fourier synthesis. Extensive research has been done in this area [10,11] since the shaping laser pulses on the femtosecond time scale was demonstrated. Recently, microstructured QPM materials have been used in ultrafast frequency conversion. QPM provides extra degrees of freedom in engineering the amplitude and phase responses for ultrafast application, a function not available with conventional birefringent phase matching. More importantly, QPM SHG devices have been used to combine such ultrafast techniques as pulse shaping and compression [12,13]. Alternatively, in this paper, we propose a frequency tripling pulse-shaping technique in a quasiperiodic LN superlattice. The characteristics of ~ 1 ps duration high-power pulse and its harmonics have been investigated numerically. Compared to the SHG, higher harmonic generations such as THG and fourth harmonic generation play a more dominant role on short pulse shaping and processing because of more interacting waves and corresponding GVM. The dependence of the temporal behavior of interacting pulses on input chirped parameter and phase mismatching detuning have been also studied. The possible physical origins of the pulse shaping and distortion, as well as the behavior of energy conversion are discussed.

Considering the classical forward propagating configuration, the nonlinear coupled equations between interacting pulses are given:

$$\frac{\partial}{\partial z}A_j(z,\Delta\omega) = -i\kappa_j \exp[i(k_j'\,\Delta\omega + k_j''\,\Delta\omega^2/2)z] \times \int \overline{P}_{NLj} \exp(-i\Delta\omega t)dt,$$

$$\overline{P}_{NL1} = E_2(z,t)E_1^*(z,t)\exp(-i\,\Delta k_1\, z) + E_3(z,t)E_2^*(z,t)\exp(-i\,\Delta k_2\, z),$$

$$\overline{P}_{NL2} = E_1(z,t)E_1(z,t)\exp(i\Delta k_1 z)/2 + E_3(z,t)E_1^*(z,t)\exp(-i\,\Delta k_2\, z),$$

$$\overline{P}_{NL3} = E_1(z,t)E_2(z,t)\exp(i\,\Delta k_2\, z),$$

$$E_j(z,\Delta\omega) = A_j(z,\Delta\omega)\exp[-ikj(\omega+\Delta\omega)z].$$

Here, $E_j(z,\Delta\omega)$ and $A_j(z,\Delta\omega)$ are the Fourier transforms of electric fields and the corresponding frequency-domain spatial envelopes, respectively. All parameters are usually defined.

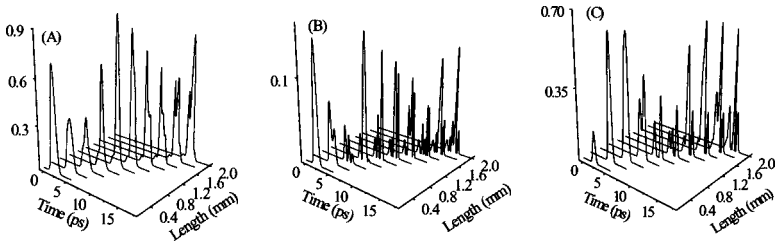

FIG. 1. Temporal distributions of fundamental (A), SH (B), and TH (C) pulses as a function of the superlattice length, respectively. An input fundamental pulse with a transform-limited Gaussian envelope is used.

Fast Fourier transform techniques and a fourth-order Runge-Kutta method are implemented to obtain the solution for the coupled equations. Convergence and stability of the numerical scheme are checked by decreasing the size of the increments of nonlinear crystal length and increasing the number of points in the discrete Fourier transform. The incident fundamental pulse used in the calculation is created by a chirped Gaussian pulse with linear chirp parameter α. Such a pulse is a good approximation to that produced by a single pulse mode-locked Nd: YAG laser system. Pulse characteristics are chosen as $I_{10}=1.0\ \mathrm{GW/cm^2}$ and pulse duration $\tau_p=1$ ps. The quasiperiodic LN structure used for simulations is the same as one introduced and studied previously [14]. It has two building blocks A and B of length l_A and l_B, which are ordered in a Fibonacci sequence.

Temporal and spectral distributions of the fundamental and harmonic pulses inside the nonlinear superlattice are shown in Figs. 1 and 2 with an input transform-limited pulse. Figures marked as (A), (B) and (C) correspond to fundamental SH and TH pulses, respectively. Here, first-order dispersive coefficients k_j' obtained from the Sellmeier equation are 7.08×10^{-9} s/m, 7.31×10^{-9} s/m and 7.66×10^{-9} s/m, respectively. Due to GVM among three interacting pulses (named multi-GVM), pulse shaping and distortion appear not only for the input fundamental but also for the generated harmonic pulses. Early in the superlattice, the TH pulse grows smoothly and reaches a maximum of conversion without pulse distortion. Structure develops in the temporal distributions after the optimum length. Some asymmetries in structure are quite apparent, especially for SH and TH pulses, which indicates that coupling of GVM δv_g^{TF} (0.58×10^{-9} s/m between TH and fundamental pulses) and δv_g^{TS} (0.32×10^{-9} s/m between TH and SH pulses) dominates for the longer superlattice lengths. An undistorted pulse is not recovered for any longer superlattice lengths, although energy does oscillate between fundamental and harmonics as the superlattice length is increased.

The fundamental pulse exhibits a simple Gaussian spec-

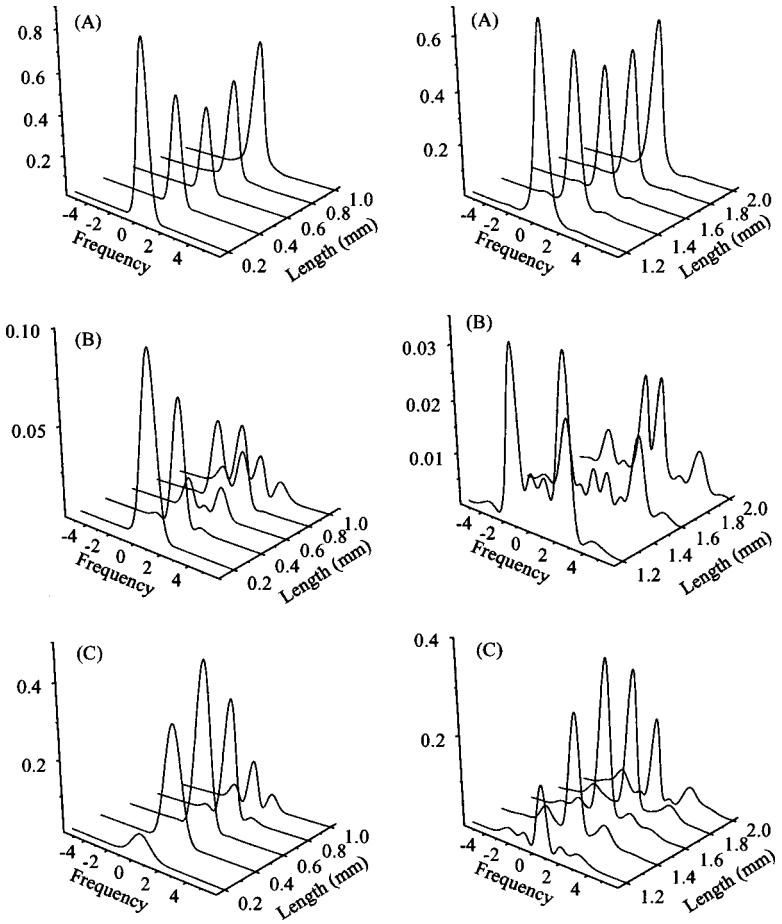

FIG. 2. Normalized spectral development of fundamental (A), SH (B), and TH (C) pulses as a function of the superlattice length, respectively. An input fundamental pulse with transform-limited Gaussian envelop is used.

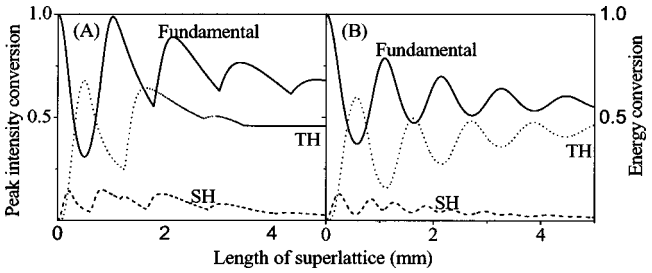

FIG. 3. Peak intensity (A) and integrated energy (B) conversions as a function of the superlattice length. Calculation parameters are the same as that in Fig. 1.

tral intensity inside the entire superlattice with negligible sidelobes. However the situations for harmonic pulses are quite different, symmetrical multiple peaked spectral structures for both SH and TH pulses occur after an optimum length (0.5 mm for the SH pulse and 0.9 mm for the TH pulse approximately). The typical spectral TH pulse shapes accompanied with strong spreading are obtained in Fig. 2(C), which are consistent with the classical physical origins conducing to a band-limiting spectral filter of $\mathrm{sinc}(x)=\sin(x)/x$ shape superimposed upon the generated TH spectrum by the GVM that is due to the phase mismatch at frequencies away from the pulse center. SH pulses with a double-peaked spectrum and a strong restriction of central spectral peak are shown in Fig. 2(B). It seems that a proper amount of quadratic phase $\exp(-ib_2\omega^2+ic_2)$ is added to generated SH spectral distributions, resulting in a strong reduction of the central spectral peak. The parameters b_2 and c_2 are determined by crystal property and pulse position inside the crystal, respectively. Because the generated SH pulse involves two processes (doubling of fundamental field and down-conversion of TH and fundamental pluses), the above results manifest that coupling and interacting of three GVM result in a simple spectral quadratic addition, which is quite similar to that induced by group velocity dispersion.

The peak intensity and integrated energy conversion inside the superlattice are plotted in Fig. 3. Both conversion efficiencies develop a kind of oscillatory behavior. There are some sharp troughs in Fig. 3(A), corresponding to the splitting into two or more intensity peaks in temporal distribution, otherwise the energy conversion revolve smoothly. It is further seen that, when the fundamental field reaches its maximum, both of the SH and TH energies decrease approximately to their minima. In particular, for a sufficiently long superlattice, SHG reaches zero and the energies of the fundamental and TH pulses converge to approximately 50% conversion efficiency asymptotically.

An incident chirped pulse can be shaped and compressed using chirped QPM superlattice [15]. It is also significant to discuss the propagations of harmonic pulses in an nonlinear quasiperiodic medium with an input chirped pulse. The corresponding numerical calculations are performed and presented. Figure 4 plots the temporal distributions of the fundamental and harmonic pulses for a positive chirp parameter ($\alpha=1.0$). Compared to the time-domain envelope of input transform-limited Gaussian pulse, there are no distinguishable differences of temporal distributions between Figs. 1 and 4 for a shorter superlattice length. There are more severe distortions for fundamental pulses in the 15 to 2.0 mm range, while the wings of the TH pulse appear to be restrained slightly for an input chirped pulse, which implies that the combination of multi-GVM among interacting pulses and an additional phase modulation induced by a chirped pulse can improve TH spectral shapes. Generally the dependences of harmonic energy conversion on the input chirp parameters are summarized in Figs. 5(A) and 5(B), corresponding to SH and TH pulses, respectively. Here, due to the simultaneous QPM in both SH and SF processes are broken, the most important feature is a reduction of THG and an increase of SHG for the input chirped fundamental pulse. The total energy conversion for harmonic generations is seen to be larger than that of transform-limited input pulse, indicating that such a quasiperiodic superlattice has a potential for simultaneously efficient SH and TH outputs pumped by a chirped fundamental pulse. Furthermore, the quantitative similarities of TH energy conversion, with respect to different input chirped parameters, for the shorter superlattice length indicate that the increase in SH energy conversion mainly results from the depletion of fundamental energy. The peaks of SH energy conversion (30%–50%) in the early superlattice appear for chirp parameters larger than 1.0, which means that SHG is more sensitive to input chirped parameters than THG in the beginning of the superlattice.

It is known that the high conversion efficiency of cascaded THG requires that the QPM conditions for both SHG and SFG are fulfilled simultaneously. However, the practical fabrications of superlattice easily generate fluctuations in the layer thickness, leading to a phase mismatch in SH and (or) SF processes. Therefore it is desirable to study frequency conversion and their pulse shaping with phase mismatch in SH and (or) SF processes. For the case that SHG is phase mismatched and SFG is phase matched, the energy conversions are illustrated in Figs. 6(A) and 6(B) for a smaller and larger SH phase mismatch, respectively. Here the SH phase mismatch is defined by the coefficient β. For the smaller SH phase mismatch, it is out of expectation that the SH energy conversion increases in comparison with perfect phase matching situation, resulting in the decrease of TH energy conversion. Both SH and TH energy conversion are rela-

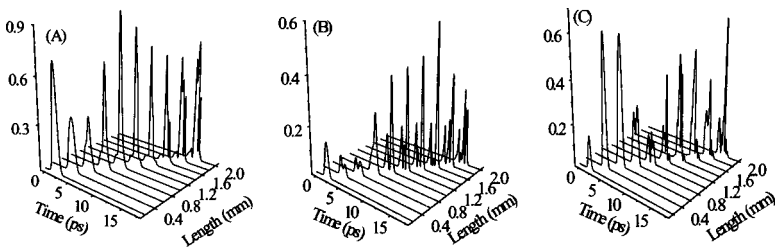

FIG. 4. Temporal distributions of fundamental (A), SH (B) and TH (C) pulses as a function of the superlattice length, respectively. An input chirped fundamental pulse ($\alpha=1.0$) is used.

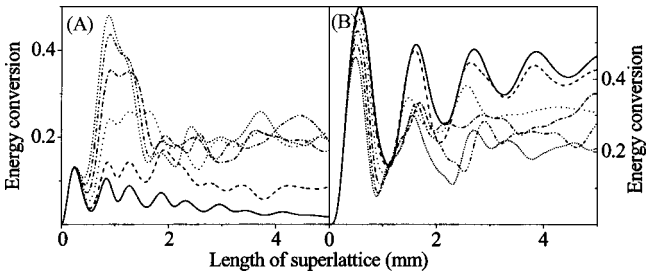

FIG. 5. Dependence of SH (A) and TH (B) energy conversions on the input chirped parameters. Solid, dashed, dotted, dash-dotted, dash-dot-dotted and short-dashed curves correspond to input chirped parameters $\alpha = 0.0$, 0.5, 1.0, 1.5, 2.0, and 2.5, respectively.

tively low for the larger SH phase mismatching, indicating that efficient THG strongly depends on not only SF process but also SH phase matching. The dependence of energy conversion with the SH phase match and SF phase mismatch are plotted in Figs. 6(C) and 6(D), corresponding to smaller and larger SF phase mismatches, respectively. Similarly, SF phase mismatch is given by β. The curves of harmonic energy conversion are slightly distorted for smaller SF phase mismatch shown in Fig. 6(C), but 40% TH output are obtained asymptotically for the longer superlattice length. From Fig. 6(D), an interesting phenomenon emerges where it is seen that efficient SHG is obtained over a wide range of superlattice when the SF phase mismatch increases and correspondingly less TH waves are generated. An efficient SH wave is seen to accumulate owing to the SH phase matching and the larger SF phase mismatch.

In this work, temporal and spectral distributions of SHG and cascade THG in a quasiperiodic optical superlattice have been studied quantitatively. Both input transform-limited and chirped pulses, as well as phase mismatching configurations in SH and (or) SF processes, are considered. Owing to multi-GVM of ultrashort pulses, pulse distortion and shaping appear. Symmetrical spectral distributions with single- and

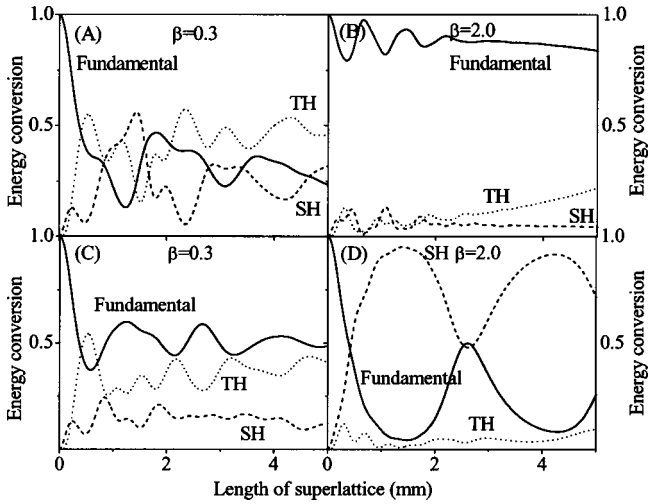

FIG. 6. Energy conversion with QPM SFG as well as (A) a smaller SH phase mismatch and (B) a larger SH phase mismatch; with QPM SHG as well as (C) a smaller SF phase mismatch and (D) a larger SF phase mismatch.

multiple-peak structures can be obtained even when their corresponding temporal envelops distort severely. SH pulses with a strong restriction of central spectral peak are observed indicating that a proper amount of quadratic phase modulation is produced due to the coupling of three GVM. There are also some interesting phenomena in energy conversion of harmonic waves in comparison with the situation of the cw wave. Through numerical optimization it is shown that improved TH energy conversion efficiency in wider regions of the superlattice can be achieved. These resulting features are seen to have an edge for practical TH conversion designs in ultrashort pulse range.

This work was supported by DSAT of Singapore under Grant No. POD0103451.

[1] D. L. Williams, D. P. West, and T. A. Ling, Opt. Commun. **148**, 208 (1998).
[2] O. Pfister, J. S. Wells, L. Hollberg, and W. R. Bosenberg, Opt. Lett. **22**, 1211 (1997).
[3] K. Kintaka, M. Fujimura, and H. Nishihara, Electron. Lett. **33**, 1459 (1997).
[4] S. N. Zhu, Y. Y. Zhu, and N. B. Ming, Science **278**, 843 (1997).
[5] L. F. Mollenauer, M. J. Neubelt, and L. G. Cohen, Opt. Lett. **15**, 1203 (1990).
[6] A. M. Weiner, in *Ultrafast Phenomena IX* (Springer-Verlag, Berlin, 1995).
[7] W. E. White, F. G. Patterson, and R. L. Shepherd, Opt. Lett. **18**, 343 (1993).
[8] D. Goswami, Phys. Rep. **374**, 385 (2003).
[9] W. S. Warren, R. Rabitz, and M. Dahleh, Science **259**, 1581 (1993).
[10] A. M. Weiner, Prog. Quantum Electron. **19**, 161 (1995).
[11] K. Ema and F. Shimizu, Jpn. J. Appl. Phys., Part 2 **29**, L631 (1990).
[12] G. Imeshev, A. Galvanauskas, and M. M. Fejer, Opt. Lett. **23**, 864 (1998).
[13] P. Loza-Alvarez, D. T. Reid, and W. Sibbett, J. Opt. Soc. Am. B **16**, 1553 (1999).
[14] Y. Y. Zhu and N. B. Ming, Phys. Rev. B **42**, 3676 (1990).
[15] G. Imeshev, M. A. Arbore, and M. M. Fejer, J. Opt. Soc. Am. B **17**, 304 (2000).